

PHOTOELECTRON SPECTRA AND BONDING IN PHOSPHORUS COMPOUNDS¹

H. Bock

Institute of Inorganic Chemistry, University of Frankfurt, (GFR)*

ABSTRACT

The results of (low energy) photoelectron spectroscopy render possible a better appreciation of bonding in molecules. The application of the new experimental method is demonstrated utilizing representative phosphorus compounds, and the close symbiosis delineated with molecular orbital models. Among the topics discussed are: the element P₄, phosphine PH₃ and derivatives, phosphorus substituent effects in organic compounds and phosphorus multiple bonding.

'Actually, everything is much more complicated'²

MOLECULAR STATES AND MOLECULAR ORBITALS

On absorption or emission of energy a molecule is transferred from one molecular state to another with different electron distribution. Measurements therefore only yield information concerning the energy difference between two molecular states and the electron distributions within them. It is the intention of the chemist to interpret and to rationalize these data, which stimulates the development and the application of simplifying models.

Although, for instance, connection lines between atoms in structural formulas are rather topological symbols, their identification with localized electron pairs has led to the conceptualization of bond models—including the definition of model quantities like covalent radii, bond enthalpies or electronegativities by artificially subdividing individual molecules into more or less independent sub-units. On the other hand, molecular orbital models—derived from linear combinations of e.g. one-electron basis functions—useful as they are for correlations with experimental data tend to over-emphasize electron delocalization. Summarizing, choosing the appropriate model³ to describe molecular states is not so much a question of verifiability but rather one of usefulness and applicability.

Photoelectron spectroscopy, the new measurement technique⁴⁻⁷ to determine all (mono) ionization potentials of chemical compounds, is based on the well-known photoionization process of a neutral species M to its radical cation M[⊕],



in which the photon energy $h\nu$ in excess of the ionization energy $IE_n(M)$

* Correspondence address: 6 Frankfurt/Main, Theodor-Stern-Kai 7.

is conserved as kinetic energy of the ejected electron

$$h\nu = IE_n(M) + E_{\text{kin}}(e^\ominus) \quad (2)$$

If one chooses—as was proposed by Turner *et al.*⁴—a helium(I) discharge lamp, for which $h\nu = 21.21$ eV, as a monochromatic photon source and counts the emitted electrons of given kinetic energy, this allows all ionization energies to be observed up to 21.21 eV

$$IE_n(M) = 21.21 \text{ eV} - E_{\text{kin}}(e^\ominus) \quad (3)$$

These ionization energies correspond to energy differences, ΔE_G , between the ground state of a molecule and its different radical cation states and can be correlated—within the restriction of unchanged geometry and other assumptions⁶—with calculated SCF orbital energies, ϵ_j^{SCF} , via use of the Koopmans theorem⁸

$$(\Delta E_{\text{total}} =)IE_n(M) \equiv -\epsilon_j^{\text{SCF}} \quad (4)$$

This relationship provides a fruitful symbiosis between photoelectron data and molecular orbital models. Generally, approximate calculations and the models deduced from them increase in usefulness the more closely they can be directly correlated with experimental data. Therefore, photoelectron spectra, which permit via the Koopmans theorem a 'quasi' reading off of orbital energies (*Figure 1*), are an exceptionally appropriate starting point for MO studies⁷.

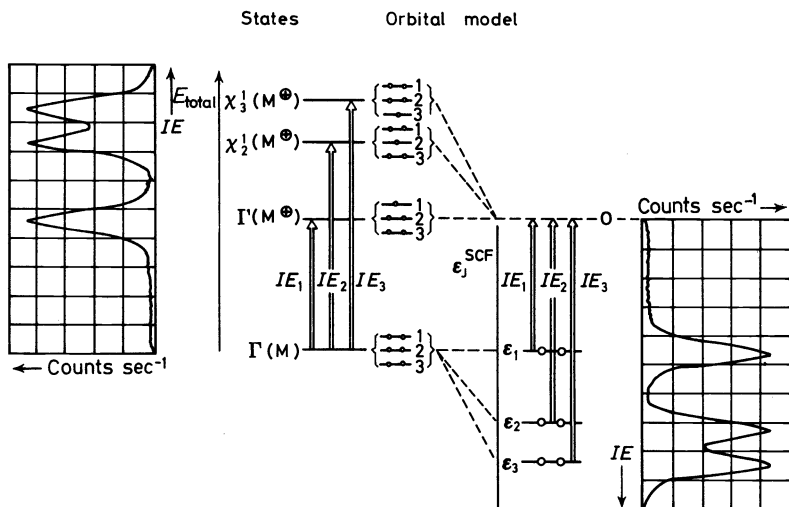


Figure 1. The Koopmans theorem: comparison of the measurable energy differences, $\Delta E_{\text{total}} = IE_n(M)$, between the molecular ground state $\Gamma(M)$ and the ground state $\Gamma(M^\oplus)$ or excited states $\chi_n^m(M^\oplus)$ of its radical cation with calculated SCF orbital energies, ϵ_j^{SCF} , (referred to the zero energy level of the removed electron).

Without diving into details unused subsequently, a few additional comments may mitigate oversimplifications. In contrast to simple MO methods,

as for example the Hückel approximation probably known to the reader, SCF calculations are carried out by an iteration process by which a part of the electron–electron repulsion can be accounted for. It is also pointed out that in the transition from the state diagram to the molecular orbital model in *Figure 1*, the states are represented in a simplified manner by a single configuration. However, a complete description of the radical cation states χ_n^m is possible only on inclusion of configuration interaction. In addition it should also be mentioned that an infinite number of sets of equivalent wavefunctions can be constructed from occupied SCF orbitals. They all yield in calculations the same total energy for a molecule. From these basis sets, the Koopmans theorem selects only the set of canonical SCF orbitals³.

In closing the above introductory remarks, it should be re-emphasized, that excitation energies to radical cation states are—via the Koopmans theorem⁸—correlated with calculations on the molecular ground state. Nevertheless, as illustrated by the following discussions of some topics, this approach adds new aspects to the description of bonding in phosphorus compounds, and with that leads also to a better understanding of other molecular properties.

THE ELEMENT P₄

The white allotrope P₄—in the gas phase a regular tetrahedron with $d_{PP} = 2.21 \pm 0.02 \text{ \AA}$ and $\angle PPP = 60^\circ$ —although first prepared in 1669, is still one of the most fascinating and perplexing phosphorus compounds. Its photoelectron spectrum (*Figure 2*) has been studied independently by several groups^{9–11}.

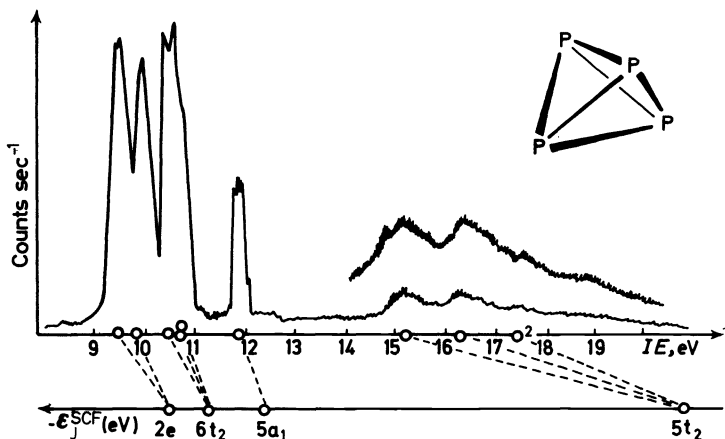
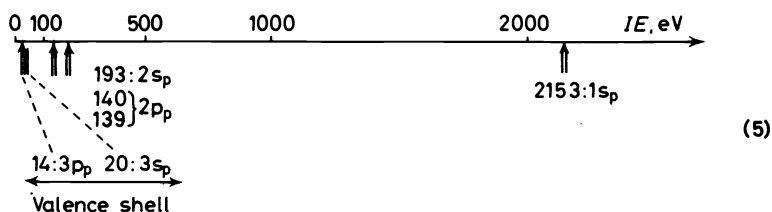


Figure 2. The helium(I) photoelectron spectrum of the P₄ molecule¹¹ with assignment according to *ab initio* SCF calculations⁹ of near Hartree–Fock limit quality.

With increasing ionization energies the P₄ PE spectrum (*Figure 2*) shows a strongly split double band followed by a less resolved band system,

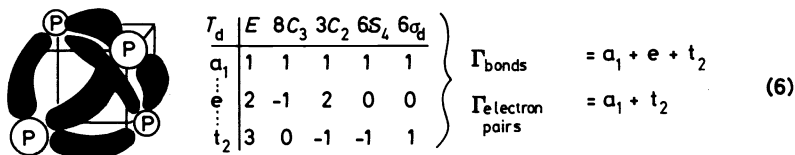
and after an isolated peak finally appears a broad ionization hill with at least one cleft. The *ab initio* calculated assignment $2e, 6t_2, 5a_1, 5t_2$ is consistent with all spectroscopic details as will be discussed later on.

To begin with, particularly for those less familiar with MO interpretations of PE spectra, a qualitative and crude model based on symmetry arguments may facilitate understanding. The first questions, how many valence shell electron ionizations are expected for the P_4 molecule and at about which energies, are answered unhesitatingly: There are $4 \times 5 = 20$ P electrons of main quantum number $n = 3$ and pairwise counting according to Pauli's principle predicts ten ionizations; scattered about $3s_p$ and $3p_p$ binding energies as determined by ESCA (Electron Spectroscopy for Chemical Analysis = high energy photoelectron spectroscopy)⁵:



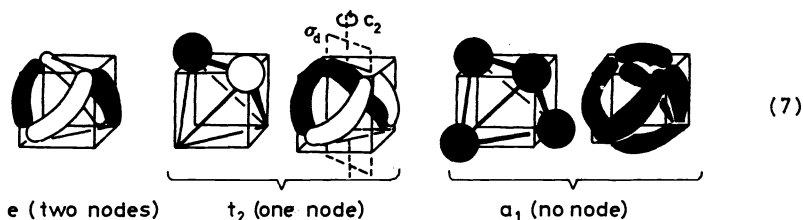
Depending upon the stabilization due to bonding, ionizations outside the helium(I) measurement range $> 21.21 \text{ eV}^3$ are possible.

The next question, how many bands should be visible in the P_4 PE spectrum, can be approached by symmetry considerations in different ways, cf. for instance in ref. 10, where linear combinations of atomic orbitals (LCAO) are chosen as the starting point to construct a qualitative molecular orbital scheme. However, more advantages are offered by a LCBO¹² (Linear Combination of Bond Orbitals) approach; because as long as unoccupied molecular orbitals play no important rôle their neglect considerably simplifies any argument. Start from a basis of six P—P bonds σ_{PP} and four phosphorus electron pairs n_p without specifying $3p_p$ contributions or $3s_p$ character, the irreducible representations, i.e. the symmetry types, of their linear combinations are easily obtained:



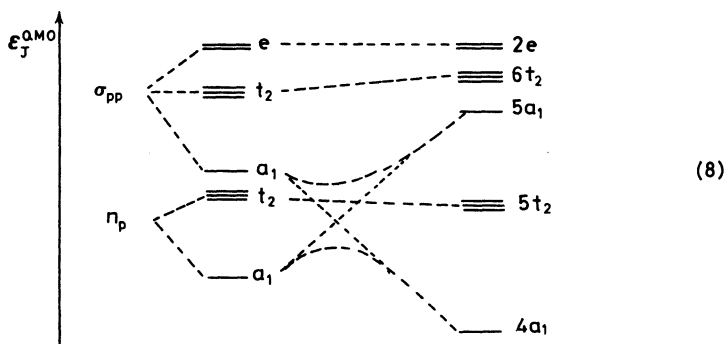
The symmetry adopted linear combinations can then be constructed using the nodal rule¹³ and again the T_d character table (6) for placing the individual nodes, e.g. t_2 orbitals must be antisymmetric with respect to the twofold axes and symmetric with respect to the diagonal mirror planes σ_d . Some

idea of what those combinations might look like, may be gathered from the sketches (7):



Within the limits of the above simple treatment—neglecting for instance Jahn–Teller distortions of the resulting radical cations—the ten valence shell ionizations are grouped into five categories. Therefore, as long as degeneracy is not removed, the twenty valence electrons of P_4 should give rise to five PE bands, of which according to scheme (5) probably four are measurable using a helium(I) source.

The final step in setting up a qualitative MO scheme requires mixing of those P–P bond and P electron pair combinations which are of the same symmetry type, i.e. the six t_2 and the two a_1 respectively:



Although the *ab initio* calculated orbital sequence (Figure 2; the numbering of orbitals, e.g. $6t_2$, refers to *all* electrons) can be easily grasped this way, the mixing of the initial combinations (7) involves changes in the components and is therefore difficult to describe within the LCBO approach. As denoted in scheme (8) by dotted lines, a special case are the two a_1 orbitals: to introduce the necessary node in the $5a_1$ molecular orbital, according to the non-crossing rule, characters of PP bonds and of P electron pairs have to be almost reversed. Thus $5a_1$ becomes more or less a non-bonding electron pair orbital and $4a_1$ a strongly bonding σ molecular orbital as is best illustrated by the *ab initio* electron density contours⁹ sketched out in Figure 3. From them one learns that the highest occupied molecular orbitals $2e$, $6t_2$ and $5a_1$

are weakly bonding or non-bonding, $5t_2$ strongly antibonding as follows from the trough at P—P midpoint and $4a_1$ strongly bonding with high electron density within the triangular face. The results suggest that the bonding in the P_4 molecule might be rationalized by overlap between the omnidirectional $3s_p$ orbitals rather than between the $3p_p$ orbitals oriented disadvantageously relative to the molecular skeleton.

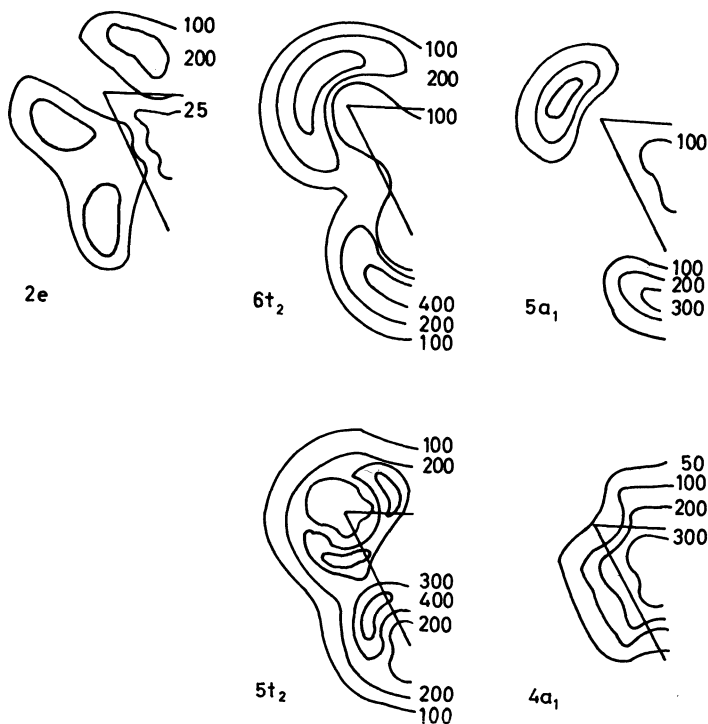


Figure 3. *Ab initio* electron density contours ($e/a_0^3 \times 10^4$) for the valence electron molecular orbitals of P_4 (high electron density close to each nucleus omitted), plotted in a plane containing a triangular face of the tetrahedron (By permission of M. B. Robin).

To what extent does the simple MO model, considerably refined by the results of a sophisticated calculation, allow one to interpret the P_4 PE spectrum? Concerning the ionization of a $5a_1$ electron, the assignment is in accordance with the observed vibrational fine structure [radical cation $\nu^\oplus \approx 560 \text{ cm}^{-1}$, neutral molecule $\nu_1(a_1) = 606 \text{ cm}^{-1}$], the small frequency decrease of the totally symmetric stretch indicating its non-bonding character. Removal of an e electron leaves the radical cation in a degenerate 2E state, subject to Jahn–Teller distortion via the e normal modes and thus explains the relatively large split $\Delta IE = 0.35 \text{ eV}$ in the first double band. The electron ejection from the second highest orbital, $6t_2$, leads to a smaller, but still recognizable split into Jahn–Teller components A and E^{9,11}. For the less

structured broad hill on the other side of the $5a_1$ band, showing at least one cleft, only the $5t_2$ assignment is left over, because ionization from the strongly bonding $4a_1$ orbital is to be expected only at much higher energy, i.e. outside the helium(I) measurement range.

Besides the conclusive assignment of the P_4 PE spectrum, there are several take-home lessons, especially from the *ab initio* calculation⁹ which far eclipses previous calculations on P_4 as regards the quality: $3s_p$ and $3p_p$ atomic orbitals are not mixed very strongly in the resulting molecular orbitals, as anticipated from the relatively large difference of the ionization potentials $IE(3s_p) - IE(3p_p)$ found in ESCA measurements (5). On the basis of the *ab initio* results, the comparable orbital sequence approximated by a simple LCBO MO model suggests its applicability for phosphorus compounds, although care must be taken in describing bonds and electron pairs. Above all, there is obviously no need to include $3d_p$ orbitals in the basis set, as long as the phosphorus valence shell has not to be expanded to incorporate multiple bonding.

PHOSPHINE PH_3 AND SOME DERIVATIVES

The garlic smelling, highly toxic phosphine is the smallest phosphorus-containing molecule stable at normal temperatures as regards its total number of eighteen electrons. The eight valence shell electrons should give rise to four ionizations, and combining qualitatively three σ_{PH} bonds plus one phosphorus electron pair n_p within the trigonal pyramidal molecular skeleton (C_{3v} symmetry), by analogy with scheme (8) one obtains an orbital

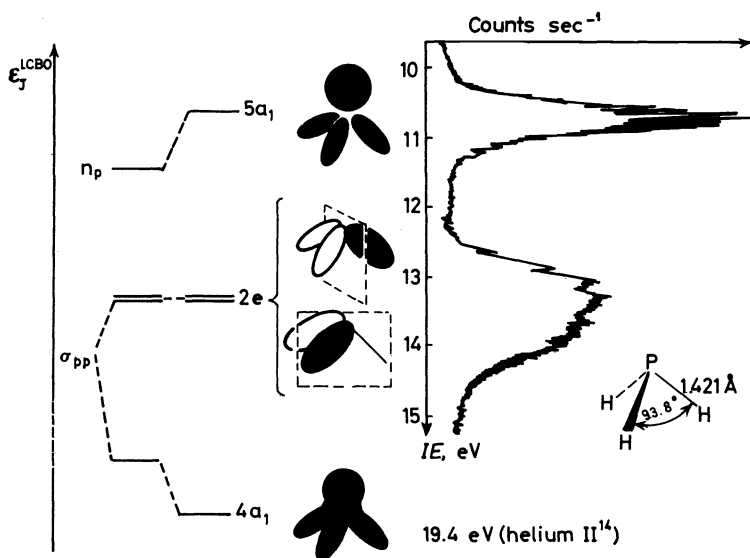


Figure 4. PE spectrum of phosphine¹⁴ and qualitative LCBO MO model.

sequence a_1, e, a_1 —numbered $5a_1, 2e, 4a_1$ with respect to the total of electrons—and therefore expects three PE bands at relatively low ionization energies.

The helium(I)^{14,15} and neon¹⁶ PE spectra of PH_3 show one single band with pronounced fine structure and one broad double band as judged from the discernible cleft, which are readily assigned to electron removal from the $5a_1$ and $2e$ molecular orbitals; the missing $4a_1$ ionization has been detected as a structureless peak in the helium(II) PE spectrum¹⁴. As for P_4 , *ab initio* calculations, e.g. refs 17–19, supply additional explanations; especially the one by Lehn and Munsch¹⁷ of near Hartree–Fock limit quality, which deals with the inversional barrier of PH_3 . Accordingly, the highest occupied molecular orbital is 88 per cent centred at phosphorus with 73 per cent $3p_p$ character and ‘thus, like NH_3 , PH_3 possesses a highly directed lone pair in contradiction to the nearly pure s type lone pair predicted by hybridization theory in view of the $93^\circ 50'$ HPH angle’. Another statement concerns the inclusion of $3d_p$ orbitals into the basis set, which ‘improves markedly the computational results although they participate only weakly in the electronic description of the phosphine molecule’; for instance, ‘the ionization potentials are left nearly unaffected’.

Both PE bands of PH_3 represented in *Figure 4* exhibit vibrational fine structure, from which further information can be gathered concerning the radical cation states resulting upon ionization. Thus, in the first PE band more than 20(!) vibrational peaks are observed with a main spacing of about 500 cm^{-1} ^{14,15}. Compared with the out-of-plane bending frequency $\nu_2(a_1) = 991\text{ cm}^{-1}$ of the neutral molecule²⁰, so-called ‘frequency halving’ takes place in the ground state of the radical cation PH_3^{\oplus} . This can be explained by a low inversional barrier, which allows the ‘left’ and ‘right’ vibrational energy levels to interact and split into equally spaced doublets (*Figure 5*, II). The angle HPH in trigonal pyramidal PH_3^{\oplus} is calculated¹⁸ to about 115° .

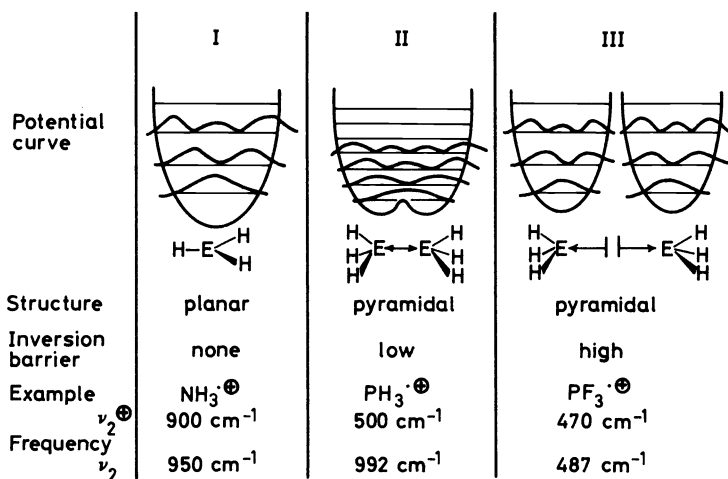


Figure 5. Different ground states (2A_1) of EX_3^{\oplus} radical cations.

In contrast, the first ionization of ammonia leads to a planar radical cation NH_3^{\oplus} (Figure 5, I) and instead of 'frequency halving' only a slight reduction²⁰ of the bending frequency $\nu_2 = 950 \text{ cm}^{-1}$ to $\nu_2^{\oplus} = 900 \text{ cm}^{-1}$ ¹⁴ is found on ejection of the only weakly bonding 'lone pair' electron.

In the second PE band of PH_3 , the vibrational progression due to the excited stretching frequency $\nu_3^{\oplus}(e)$ breaks off at about 13.4 eV^{14, 15}, near the appearance potential for the fragment ion PH_2^{\oplus} . This predissociation $\text{PH}_3^{\oplus} \rightarrow \text{PH}_2^{\oplus} + \text{H}^{\cdot}$ is in accordance with the ionization of a σ_{PH} bonding electron and confirms—together with the cleft at about band midpoint due to Jahn–Teller distortion of the corresponding radical cation which removes the degeneracy of the e orbitals—the assignment proposed in Figure 4.

Based on the detailed discussion of the parent molecule, PH_3 , some excursions to chemically related compounds may add further aspects. To begin with, valence shell PE ionization potentials^{14, 4, 7} for species isoelectronic with PH_3 are correlated horizontally and vertically within the periodic table (Figure 6).

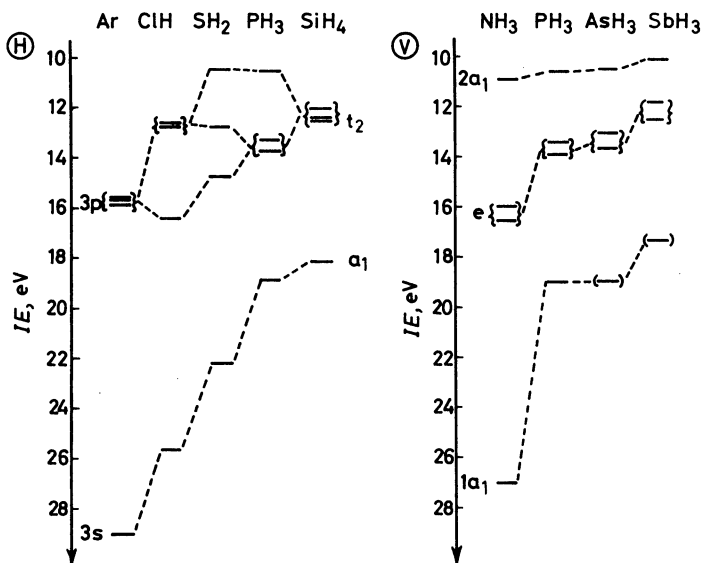
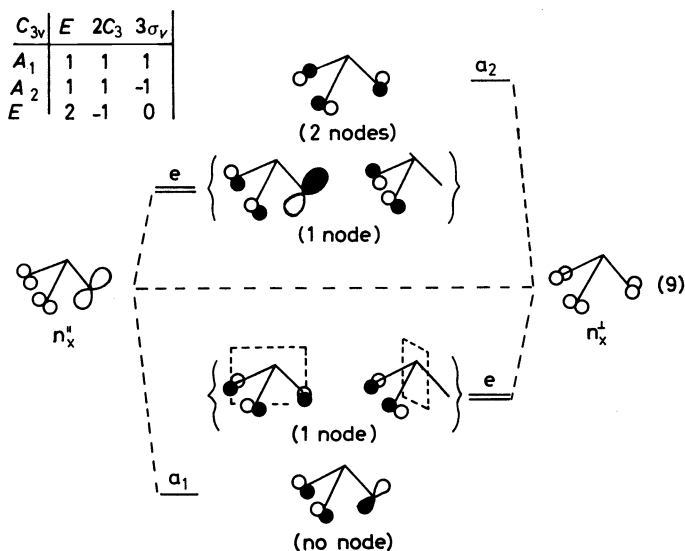


Figure 6. Correlations of valence shell PE ionization potentials around PH_3 within the periodic table. Horizontally \textcircled{H} , a 'united atom' approach¹⁴ for hydrides EH_x of elements E with main quantum number 3 and vertically \textcircled{V} , comparing the group Va element hydrides EH_3 ¹⁴.

The 'united atom' approach, i.e. the progressive displacement of unit positive charge from the argon nucleus, thereby reducing the number of lone pairs n_E and increasing the number of σ_{EH} bonds, leads to the splitting patterns of the individual element hydrides¹⁴ governed by their molecular symmetry (Figure 6, \textcircled{H}). The 3s shell of argon passes continuously through the series to the a_1 shell of silane; the decreasing ionization thereby reflecting to some extent the decreasing effective nuclear charge. The 3p degeneracy

of argon is completely removed in H_2S , and formally two of its σ_{SH} orbitals mix to generate the $\sigma_{\text{PH}}(2e)$ orbitals of PH_3 at an intermediate ionization potential. The phosphine electron pair n_p is a little stabilized by σ contributions (Figure 4), relative to the pure lone pair⁷ n_s . Finally, moving the fourth hydrogen unit out of the former argon nucleus, n_p and σ_{PH} components are transformed into the triply degenerate σ_{SiH} bonding orbital t_2 of silane, again at about an intermediate ionization energy. The vertical correlation between the element hydrides EH_3 ¹⁴ (Figure 6, ⊙), in which the centre of gravity as well as individual ionization energies decrease, demonstrates even more convincingly the governing influence of diminishing effective nuclear charge. Only the outermost electrons are relatively unaffected (Figure 6, orbitals $2a_1$), an astonishing observation in view of the molecular differences as documented by the varying HEH bond angles (NH_3 107.8° , SbH_3 91.3° ²¹). Discussions of the complex pyramidal inversion process^{17,22} demonstrate that model terms like bond/bond repulsion^{21b} or substituent electronegativity²² as well as a hybridization description^{17,23}, rationalize only partial aspects. Thus, although the first ionization energies of the hydrides EH_3 (Figure 6, ⊙) are within the narrow range of 0.8 eV, there are characteristic differences in the resulting radical cation states (2A_1): only that of NH_3^{\oplus} is planar (Figure 5, I), while all the others are trigonal pyramidal¹⁴, showing 'frequency halving' (Figure 5, II).

Extension of the PH_3 orbital model (Figure 4) for phosphorus halides PX_3 can be achieved in a simplified manner by subdividing the additional 6 p-type electron pairs n_x , which have to be considered, into those parallel (symmetric) n_x^{\parallel} and those perpendicular (antisymmetric) n_x^{\perp} to the three mirror planes of the C_{3v} point group. Their independent linear combinations are spread around the centre of gravity n_x according to the number of nodes.



This qualitative approach and the underlying assumptions are easily tested, for example, looking at the PE spectrum of PF_3 ^{24, 25} (Figure 7): the mean ionization energies $n_F^\parallel = (6e + 7a_1)/3 \sim 17$ eV and $n_F^\perp = (1a_2 + 5e)/3 \sim 17$ eV not only correspond to each other but roughly also to the $IE(2p_F) = 17.4$ eV of fluorine atoms. The same is valid for the n_x ionization energies of PCl_3 and PBr_3 as assigned in ref. 25. In the latter, due to the decreasing atomic potentials $IE(3p_{Cl}) = 13.0$ eV $>$ $IE(4p_{Br}) = 11.8$ eV around which the splitting (9) occurs, the bromine lone pair combination $n_{Br}(1a_2)$ emerges as the highest occupied orbital for phosphorus tribromide—about 1.2 eV easier to ionize than the phosphorus electron pair n_p ²⁵.

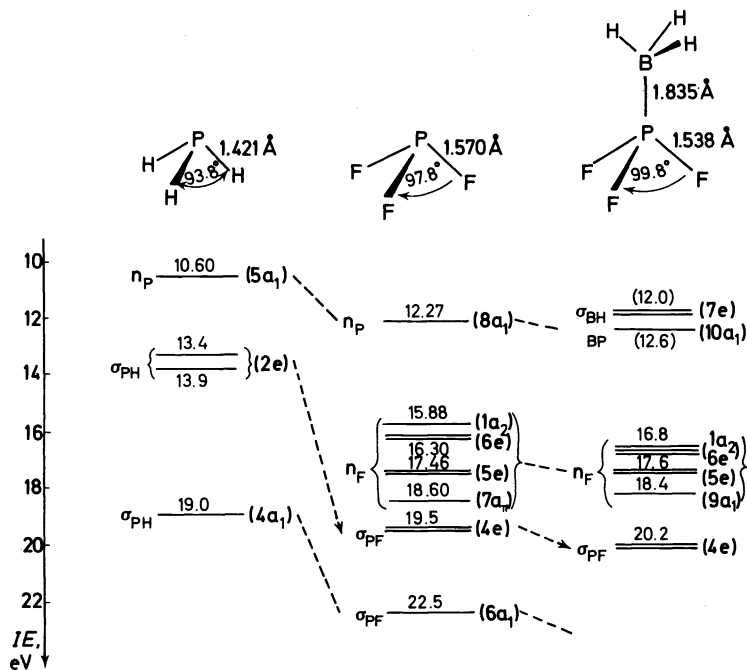
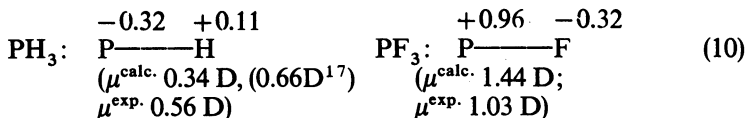


Figure 7. Correlation of ionization energies in the series H_3P ¹⁴, F_3P ^{24, 25} and F_3PBH_3 ²⁶ and assignment of their photoelectron spectra.

The assignment of the PF_3 photoelectron spectrum^{24, 25} given in Figure 7 can be supported by numerous observations and arguments. Thus, besides the above correlation with other phosphorus trihalides an even more convincing comparison with the NF_3 ionization potentials²⁴ yields not only identical splitting patterns but especially in the n_F region an almost 1:1 correspondence. A pronounced vibrational progression of more than twenty peaks appears again in the first PE band (Figure 5, III)¹⁵, but contrary to NH_3^\oplus and PH_3^\oplus a trigonal pyramidal structure with high inversional barrier is proposed on the basis of *ab initio* calculations¹⁸ which yield for the phosphorus electron pair 35 per cent $3p_p$ and 35 per cent $3s_p$ contributions. This

result interprets in hybridization terms the increase in n_p ionization potential caused by H/F exchange in phosphine derivatives independently from angle opening (Figure 7), and fits also in the rationalization of higher inversional barriers with stronger electron-withdrawing substituents^{17, 22}. Most impressive in the correlation PH_3/PF_3 , however, is the 5 eV difference in ionization potentials between σ_{PH} and σ_{PF} bonding ^2E states as well as the 3.5 eV difference for the $^2\text{A}_1$ states. The *ab initio* calculated total charges¹⁸,

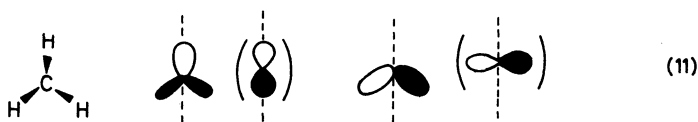


supported by good agreement between experimental and calculated dipole moments¹⁸, suggest considerable electron density transfer towards the fluorine ligands—not only explaining the decrease in n_p ionization potentials relative to the atomic value, but also strengthened bonding within the σ skeleton as absorbed in the commonly used bond parameters $\Delta Hb_0^{298}(\text{P—H}) \sim 76$ kcal/mole and $\Delta Hb_0^{298}(\text{P—F}) \sim 117$ kcal/mole.

To round off the comments on photoelectron spectrum and bonding in PF_3 , structural changes on complex formation $\text{F}_3\text{P} \rightarrow \text{F}_3\text{PBH}_3$ will be discussed within another useful model which rationalizes molecular geometry in terms of electron-pair repulsion (cf. R. J. Gillespie^{21b}). Being most successful in predictions of the overall polyhedral arrangement around the central atoms under consideration, sometimes it can even comprehend features which concern delicate charge balance changes within the series of related molecules. On addition of BH_3 , which stabilizes the PF_3 electron pair n_p by forming a σ_{BP} bond (Figure 7), simultaneously the angles FPF open and the PF bonds shorten. These findings can be interpreted as follows. Generally, the higher the overall electron density around the central atom E of a trigonal pyramid EX_3 , the stronger are the repulsions between the adjacent E—X bonds and between the E—X bonds and the electron pair n_p —for example, the angles HEH decrease from NH_3 to SbH_3 or the angles XPX increase from PH_3 to PF_3 (Figure 7). Withdrawal of electron density from around the central P atom by transforming n_p into σ_{BP} , therefore, should not only open the FPF angles due to smaller $\sigma_{\text{BP}}/\sigma_{\text{PF}}$ repulsions, but also shorten the PF bonds because the enhanced acceptor properties of the central P counteract the electron withdrawal towards the fluorine ligands^{21b}. Looking again at the PE spectrum of the Lewis acid/base adduct²⁶, as expected from the above argument, the mean ionization energy n_p is increased relative to that in PF_3 (Figure 7). Analogous changes in ionization potentials for $n_p \rightarrow \sigma$ and some Δn_p , are reported for metal complexes like $\text{Ni}(\text{PF}_3)_4$ ²⁷, in which the P—F bonds are shortened to 1.561 Å.

In reviewing the numerous arguments for PF_3 , independent of whatever model seems appropriate to describe a partial aspect, it is the comparison of photoelectron spectra of related compounds which yields interesting information for the chemist (cf. Figures 5, 6 and 7). Thereby, the selection of a series of molecules for comparison is rather a matter of the relationship to be emphasized. If one likes, for instance, to compare axially symmetric substituents with the same number of seven valence electrons, then fluorine

ligands and methyl groups offer some resemblance, if the CH bonds are combined into group orbitals symmetric or antisymmetric to mirror planes:



Although it might seem exaggerated to stress the isoelectronic concept that much, this approach facilitates following the assignment of the trimethyl phosphine PE spectrum^{23, 28, 29} (Figure 8) based on *ab initio* SCF calculations^{18, 30}. The first single band, denoted n_p , is due to ionization from an orbital 81 per cent localized at phosphorus with 67 per cent $3p_p$ character¹⁸. The second band of doubled intensity represents the $\sigma_{PC}(e)$ bonding orbital, raised about 2 eV relative to $\sigma_{PH}(e)$ of PH_3 (Figure 4) and about 8 eV relative to $\sigma_{PF}(e)$ of PF_3 (Figure 7). The broad hill centred at about 14.25 eV²⁹, the value for e-type methyl group ionizations³¹, contains at least four overlapping bands, which—according to the isoelectronic concept (11)—can be assigned to electron removal from the σ_{CH} orbitals $1a_2$, $5e$, $4e$ and $7a_1$, resembling those sketched out for the n_F combinations in (9).

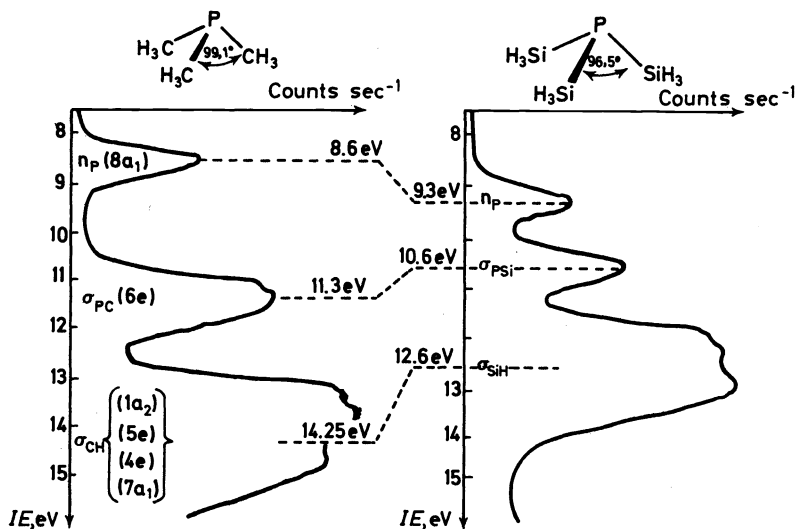
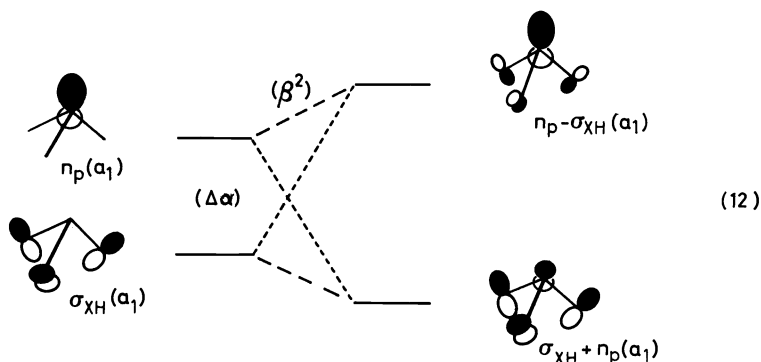


Figure 8. Comparison of the helium(I) PE spectra between 8 and 16 eV of trimethyl and trisilyl phosphine^{29, 32}.

The lower energy part of the trisilyl phosphine PE spectrum^{29, 32} (Figure 8) shows essentially the same features as the one of the trimethyl derivative and is consequently assigned using the same orbital sequence. However,

considerable band shifts are observed, which can be explained in different ways within the framework of different models^{31, 33}. Because bond orbital descriptions, which only take into account occupied orbitals, are more translucent and easier to handle, and because no $3d_p$ participation^{29, 33} has been absolutely required so far in the discussion of three- or four-coordinated phosphorus compounds, a hyperconjugation approach, e.g. refs. 7, 23, 31, will be preferred. It consists in mixing so-called basis orbitals of the same symmetry type, for instance $n_p(a_1)$ and $\sigma_{XH}(a_1)$, the latter one symbolized in (11) by the corresponding p_x atomic orbitals:



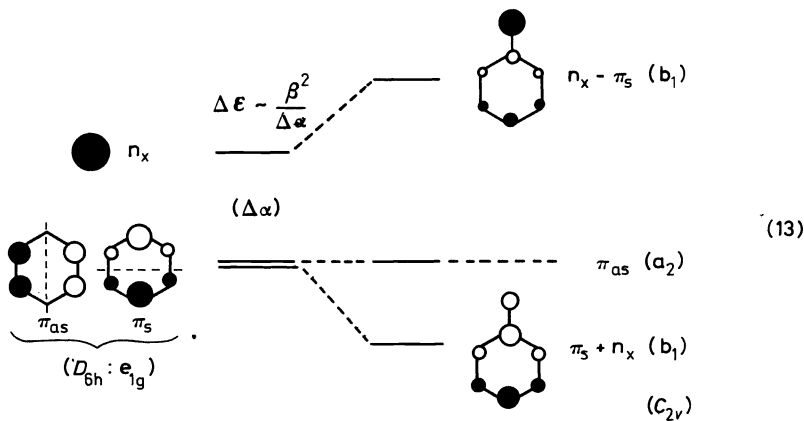
The linear combinations formed—the negative one depicting the ‘lone pair’ destabilized by antibonding σ_{XH} admixture and the positive one displaying a σ_{XH} bonding orbital, further stabilized by a bonding n_p contribution—represent a substantial refinement of simple models towards the results of sophisticated calculations, which allows us to attribute so and so much character to, say, the phosphorus ‘lone pair’. The split itself is proportional to the square of the interaction parameter β (resonance integral) and inversely proportional to the orbital distance $\Delta\alpha$ (Coulomb integral difference). Returning to the trimethyl and trisilyl phosphine PE spectra (Figure 8), both σ_{PSi} and σ_{SiH} ionization are shifted to lower energies as expected from the reduced effective nuclear charge of silicon (cf. Figure 6), whereas the 0.7 eV increase of the n_p ionization energy can be rationalized within a hyperconjugation model (12) by a reduced interaction parameter $\beta_{P/SiH_3} < \beta_{P/CH_3}$ ³¹. The overall electron release from the silicon atoms to the central phosphorus is compatible with other findings: thus the reduced SiPSi angle (Figure 8) would fit into the electron pair repulsion model as discussed for the F_3PBH_3 complex formation (Figure 7), if caused by increased n_p/σ_{PSi} repulsion. Also, the considerably lowered inversion barrier—for $P(SiH_3)_3$ estimated to be ~ 10 kcal/mole relative to ~ 36 kcal/mole measured for trialkylphosphines²²—follows generalizable trends^{17, 22} as discussed for electron withdrawal in PF_3 . If, finally, the difference in effective nuclear charges becomes too large, the inversion barrier approaches zero and geometry alterations take

place as, for example, in the isosteric pairs³³ $\text{H}_3\text{COCH}_3 \rightarrow \text{H}_3\text{SiOSiH}_3$ with an angle SiOSi 144.1° versus $\text{H}_3\text{CSCH}_3 \rightarrow \text{H}_3\text{SiSiSiH}_3$ with an angle SiSiSi 97.4° or, in connection with the above example $(\text{H}_3\text{C})_3\text{P} \rightarrow (\text{H}_3\text{Si})_3\text{P}$, between pyramidal $(\text{H}_3\text{C})_3\text{N}$ and planar $(\text{H}_3\text{Si})_3\text{N}$ ^{29, 32}.

PHOSPHORUS SUBSTITUENT EFFECTS IN ORGANIC COMPOUNDS

Stimulating as it might be to continue the report on photoelectron spectra and bonding for the simpler phosphine derivatives, the aspects elaborated in the preceding section nevertheless permit consideration of some details in larger and more complex organosphosphorus molecules. In the following, two of the known examples are chosen, namely the π perturbations of a benzene ring by 'outside' phosphine groups and by 'inside' phospho-substitution.

Usually, substituent effects on the benzene π system are approximated by a second-order perturbation approach, e.g. refs. 13, 34–36, considering only the highest occupied orbitals, i.e. the electron pair n_x and the benzene orbitals ($D_{6h}:e_{1g}$) π_{as} (node through centres) and π_s (node through bonds).



The bird's eye view molecular orbital diagrams indicate that as in the hyperconjugation model (12) only basis orbitals of same type will mix, i.e. in mono-substituted benzene derivatives of C_{2v} symmetry linear combinations $n_x \pm \pi_s(b_1)$ have to be formed, while $\pi_{as}(a_2)$ remains conjugationally unaffected. Again, as in scheme (12), the split is proportional to the interaction parameter (β^2) and inversely proportional to the distance ($\Delta\alpha$) between the mixing orbitals. Photoelectron spectroscopy, yielding all ionization energies is well suited for checking the expected perturbation patterns, whenever the corresponding PE bands are separated^{35, 36}. Unfortunately, phenylphos-

phine derivatives show in their 7–11 eV PE spectral regions a poor disentanglement of the overlapping bands^{37–39}—contrary to those of the corresponding anilines^{36–39} which therefore offer the decisive clues for the interpretation (*Figure 9*). However, before entering any tentative interpretation, attention has to be drawn to the fact that the ionization potentials reported^{36–39} sometimes deviate considerably from each other. Nevertheless, consistent splitting schemes can be derived with the values^{36,37} given in

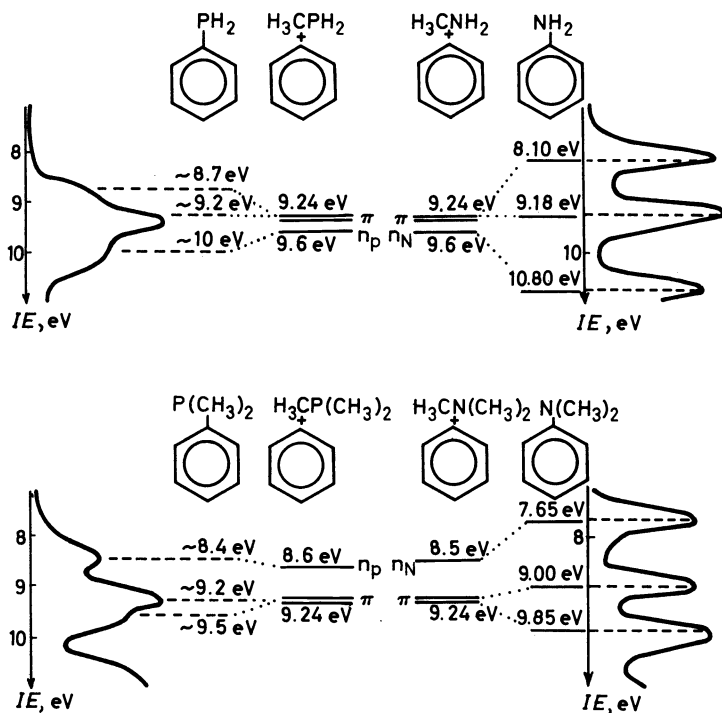


Figure 9. PE band patterns 7–11 eV for phenylphosphine, aniline and their dimethyl derivatives with a tentative explanation by perturbation arguments^{36–39}.

Figure 9 under the assumption that the first ionization potentials of the methyl derivatives H_3CXH_2 and $\text{H}_3\text{CX}(\text{CH}_3)_2$ are representative standards for the electron pair basis orbitals n_{X} . Obviously, the split π/n_{P} is smaller than π/n_{N} as is also found in more clear-cut comparisons of isosteric second and third row element compounds, e.g. $\Delta IE(\pi/n_{\text{O}}) = 1.35$ eV versus $\Delta IE(n_{\text{S}}/\pi) = 0.82$ eV³⁵ or $\beta_{\pi/\text{CH}_3} = -2.07$ eV versus $\beta_{\pi/\text{SH}_3} = -1.25$ eV³¹. The resulting molecular orbitals are comparatively mixed³⁶ and are better not classified³⁸ further according to their origin. In conclusion: for dimethylaniline a planar π system with an angle $(\text{H}_3)\text{CNC}(\text{H}_3)$ of 116° has been determined by electron diffraction^{21a}; the dimethylamino substituent effect shifting π_{as} from 9.24 eV to 9.00 eV (*Figure 9*) points to limits of the perturbation model (13) as dis-

cussed later on for the ylides, and, an investigation of the 1,4 disubstituted derivatives might offer some clues not only because of increased splitting, but rather because the electron pair combination n_x^+ establishes an internal standard^{7, 35, 36}, relative to which the perturbation schemes (*Figure 9*) can be calibrated.

For an illustration of the alternative possibility of perturbing the benzene π system in organosphorus compounds, namely the 'inside' phospho-substitution, one of the exemplary collaborations of preparative, physical and theoretical chemists can be quoted⁴⁰: phosphabenzene⁴², synthesized

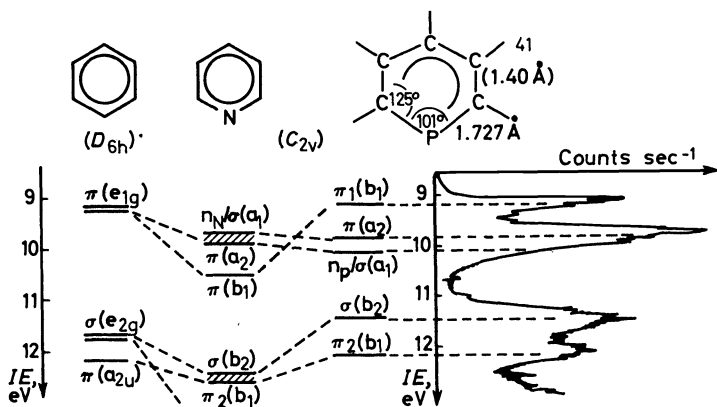
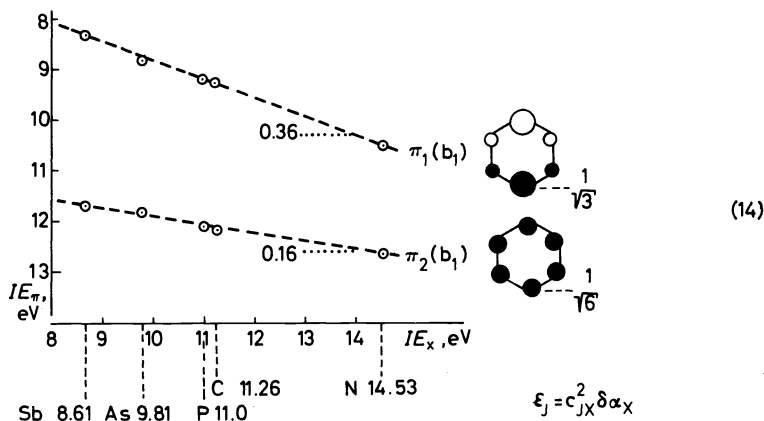


Figure 10. Phosphabenzene PE spectrum 8.5–13 eV and correlation of ionization energies with those of pyridine and benzene⁴⁰.

substituent-free^{40, 41} only in 1971, is the simplest isosteric benzene derivative imaginable. Its PE spectrum (*Figure 10*) consists of well separated bands, and there is no question concerning the assignment supported by an *ab initio* calculation⁴⁰. As in pyridine, the 'lone pair' is part of the planar σ skeleton and the corresponding orbital therefore denoted $n_p/\sigma(a_1)$. In C_{2v} molecules, the π orbitals usually belong to either the a_2 or the b_1 symmetry species (cf. scheme (13): π_{as} and π_s), and starting from the three occupied π orbitals of benzene, e_{1g} and a_{2u} , the latter one also adopts b_1 behaviour if the overall symmetry changes from D_{6h} to C_{2v} on substitution (*Figure 10*). Inserted between the π molecular orbitals is another σ orbital, twofold degenerate in benzene (e_{2g}) and single (b_2) in pyridine and phosphabenzene. The π orbital correlations in *Figure 10* can be rationalized by first-order perturbation¹³, according to which the shift $\delta\epsilon_i$ of an orbital ψ_i by perturbation $\delta\alpha_x$, i.e. a change in the basis orbital energy α_x , is proportional to the square of the coefficient c_{jx}^2 at the substitution centre X as presented in the following diagram:



On extension of the series to include also arsabenzene and stibabenzene⁴⁰ linear regressions between each of the $\pi(b_1)$ ionizations and the first atomic ionization energies IE_X become manifest. The individual slopes of the regression lines, 0.36 for $\pi_1(b_1)$ and 0.16 for $\pi_2(b_1)$, from in perfect accord with the first-order perturbations as expected from coefficients c_{jX} for the two benzene $\pi(b_1)$ orbitals, $1/\sqrt{3}$ for $\pi_1(b_1)$ and $1/\sqrt{6}$ for $\pi_2(b_1)$, respectively⁴⁰. On the contrary, little change in orbital energy is anticipated for $\pi(a_2)$ with a node passing through the substitution centre X [cf. scheme (13) and Figure 9], and consistently the double band—containing also the n_X/σ ionization in unknown ordering—barely moves on $N \rightarrow P \rightarrow As \rightarrow Sb$ exchange⁴⁰. In conclusion, attention is drawn to the results of the *ab initio* calculations, according to which inclusion of $3d_p$ orbitals into the basis set 'is unimportant in understanding structure and bonding in phosphabenzene'⁴⁰, as well as to the compatible sequence of the upper three orbitals independently proposed for the more complex PE spectrum of 2,4,6-tri-tert.-butylphosphabenzene⁴³.

Summarizing, artificial as the subdivision of individual molecules into parent systems and substituents may be, its justification rests mainly on the benefit in rationalizing and comparing numerous properties of numerous compounds. Therefore it is good to know that first and second-order perturbation arguments—illustrated above for phosphabenzene and phenylphosphines—can also be applied to organophosphorus derivatives. Any further subdivision of the overall substituent effects—e.g. into inductive, hyperconjugative or $p_\pi d_\pi$ back bonding components—is rather a question of usefulness or applicability of the model under consideration than of its verifiability: experimental data can neither prove nor disprove their 'semantic' presence^{31, 44}.

PHOSPHORUS MULTIPLE BONDING

The PE spectrum of phosphabenzene, a Hückel type $(4n + 2)$ π system containing phosphorus, has been interpreted emphasizing first-order pertur-

bation arguments [Figure 10 and Scheme (14)]. Continuing the discussion of phosphorus multiple bonding, i.e. π interactions perpendicular to the σ skeleton, it seems advisable to distinguish between less than four-coordinated phosphorus centres and those which are formally surrounded by more than eight valence electrons.

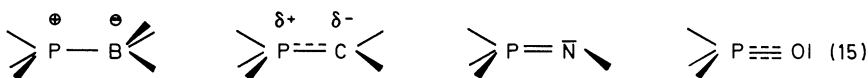
Passing phosphine through a low-intensity rotating arc struck between carbon electrodes yields—besides acetylene as main product— $\text{H}-\text{C}\equiv\text{P}^{45}$, one of the most fabulous phosphorus compounds, stable for a few hours at room temperature. From the skilfully recorded PE spectrum of the reaction mixture⁴⁶, two bands exhibiting vibrational fine structure are unequivocally assigned to methinophosphide ionizations (Figure 11).

$\begin{array}{c} 1.06\text{\AA} \quad 1.54\text{\AA} \\ \text{H}-\text{C}\equiv\text{P} \end{array}$		$\begin{array}{ccc} +0.23 & -0.31 & +0.08 \\ \text{H} & \text{C} & \text{P} \\ 0.77 & 1.62 & \\ \mu^{\text{calc.}} & >0.11 & \text{D} \end{array}$	
$\mu^{\text{exp.}}$	0.39 D		
IE_n (eV)	ν^\oplus (cm ⁻¹) ⁴⁶	$-\epsilon_j^{\text{SCF}}$ (eV)	Orbital character ⁴⁷
10.79	1100	9.5	$\pi_{\text{C-P}}$
12.86	1250	12.5	$\pi_{\text{P-}\sigma}$
	($\nu = 1270$)	19.2	σ_{CH}
		25.8	σ_{PC}
		145.5	2p _P
		145.6	2s _P
		204	2s _C
		309	1s _C
		2176	1s _P

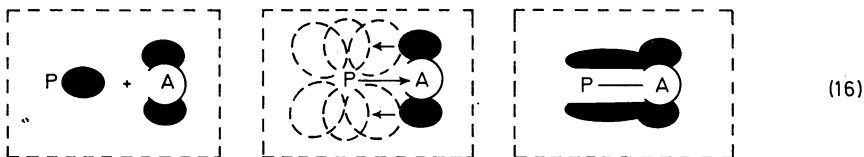
Figure 11. Comparison of experimental⁴⁶ and calculated⁴⁷ data for methinophosphide.

A series of *ab initio* calculations with different basis sets had been carried out two years earlier⁴⁷. The resulting eigenvalues $-\epsilon_j^{\text{SCF}}$ predict fairly well via Koopmans theorem $-\epsilon_j^{\text{SCF}} = IE_n$ the ionization energies, including the ESCA data for inner-shell electrons [Scheme (5)]. Additional evidence for correct orbital assignment can be gathered from the reduced stretching frequency in the radical cations HCP^\oplus relative to the neutral molecule: $\Delta\nu \sim 170 \text{ cm}^{-1}$ on removal of a π bonding electron, and $\Delta\nu$ only $\sim 20 \text{ cm}^{-1}$ after ionization of the almost non-bonding phosphorus electron pair (Figure 11). Even more impressive, the experimental gas-phase dipole moment is almost reproduced by the calculation, lending credit to the Mulliken population analysis for HCP^{47} on the right-hand side of Figure 11: accordingly, the CP bond is less polarized than the CH bond, and its overlap population is almost three times as high. Therefore, within the chemical short-hand bond notation a triple connection line seems appropriate, namely $\text{H}-\text{C}\equiv\text{P}$.

Phosphorus multiple bonding as in phosphabenzene or methinophosphide, where the π systems are easily constructed using the singly occupied $3p_p$ orbitals, does not necessarily imply $3d_p$ participation. But even if the formal number of valence electrons around a third row element in one of its compounds exceeds that of the argon shell, it is still questioned⁴⁴ whether $3d$ or $4s + 4p$ atomic orbitals will be best suited to enlarge the basis set needed for the MO calculation. However that may be, the virtual $3d_p$ orbitals are most popular for improving the bonding description in molecules with 'phosphorus (+5) of coordination number 4', in which contrary to, say $\text{H}-\text{C}\equiv\text{P}$, the varying bond order down an isoelectronic series can hardly be covered by the usual notation:



C_{3v} molecules with axial symmetry along the phosphorus multiple bond are easiest to begin with. In an imaginary way, they can be composed of a phosphine donor and an acceptor group or atom. This 'molecules in molecule' approach may be further simplified by stepwise assemblage as viewed in a paper-plane cut:



The excessive charge inflicted upon the acceptor A in σ complex formation is partly retransferred to the phosphine donor via ($p_A \rightarrow d_p$) and ($p_A \rightarrow p_p$) π back donations. Thereby, a more balanced charge distribution is achieved, which stabilizes the molecule and corresponds to a multiple bond PA—varying, of course, from compound to compound. To what extent can this commonly used model be supported by combined results of PE spectroscopy and MO calculations? Continuing the discussion²⁶ of the adduct F_3PBH_3 (Figure 7), the F_3P ionization energies^{24, 25} are also helpful in assigning^{24, 48} the PE spectrum of its oxygen adduct, F_3PO ^{24, 49} (Figure 12). In the correlation $\text{F}_3\text{P} \rightarrow \text{F}_3\text{PO}$, only smaller changes in energy and composition are expected for n_F and σ_{PF} orbitals, and, after identifying the first PE band of double intensity with the π stabilized [Scheme (16)] oxygen electron pairs, only the 15.68 eV ionization remains for the σ_{PO} bond. Accordingly, the stabilization $n_p \rightarrow \sigma_{PO}$ amounts to more than 3.3 eV [cf. Scheme (16) and Figure 12], whereas on F_3PBH_3 complex formation a difference $IE(\sigma_{BP})$

$-IE(n_p)$ of only about 0.4 eV is observed. This finding suggests that the oxygen atom is a more powerful σ acceptor than the borine group—in accordance with further angle opening and bond shortening in F_3PO relative to the geometry changes already discussed for $F_3P \rightarrow F_3PBH_3$. On the other hand, the ' n_o ' ionization energy seems rather high if compared—with some reservation—to $IE_1(b_1) = 12.6 \text{ eV}^7$ for the oxygen electron pair of water. This difference indicates considerable π back donation to phosphorus [Scheme (16)] in full agreement with the exceptionally large PO force constant $f_{PO} = 11.38 \text{ m dyn/\AA}^{50}$ of F_3PO . As is evident from the above arguments, however, unambiguous standards are missing on which a comparison of the different molecules under consideration can be based. Fortunately, detailed *ab initio* calculations have been carried out⁵¹, some results of which are summarized in Scheme (17), and which fully support the con-

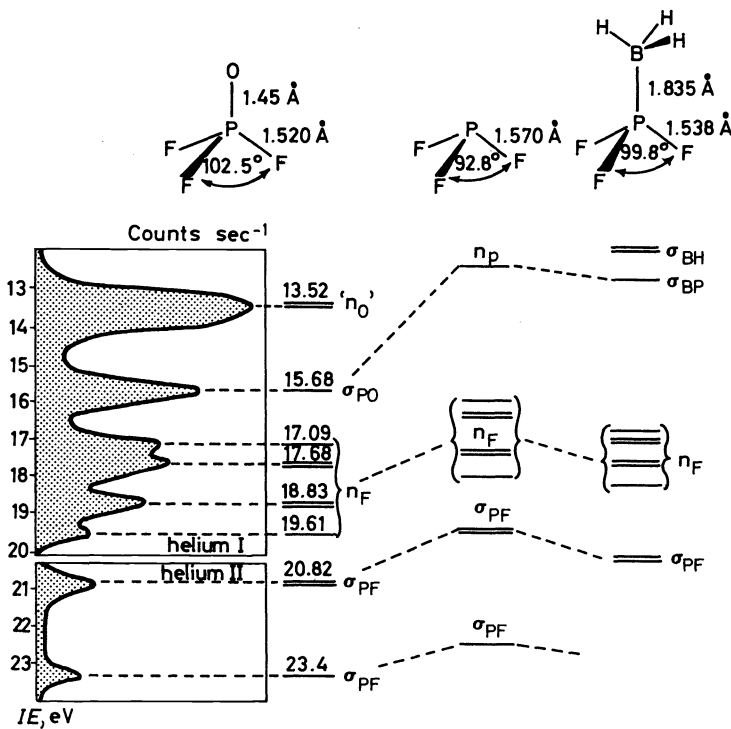


Figure 12. PE band pattern and ionization energies²⁴ of F_3PO compared to those of F_3P ²⁴ and F_3PBH_3 ²⁶.

clusions drawn from the PE spectra (Figure 12). On complex formation, the total charges show a small decrease at the negative fluorine ligands and a larger increase at the positive phosphorus centre, which can be proved experimentally by increased $2p_p$ binding energies⁵² from ESCA measurements (5).

The combined negative charge of the borine group exceeds that at the oxygen atom:

	$\text{F}-\text{P}$	$\text{F}-\text{P}-\text{B}-\text{H}$	$\text{F}-\text{P}-\text{O}$	
total	-.34	-.31	-.32	
charges	+1.02	+1.16	+1.11	
		{ +.12 }		
		- .23		
			(17)	
overlap popula- tions	{	σ 0.46	0.57	0.56
		$\pi(\text{p})$ 0.07	0.08	0.37
		$\pi(\text{d})$ 0.19	0.08	0.54
	total	0.72	0.73	1.47

But it can be deduced from the overlap populations, contrary to F_3PBH_3 , that for F_3PO an enormous charge balance via $(p_{\text{O}} \rightarrow 3p_{\text{P}})\pi$ and especially $(p_{\text{O}} \rightarrow 3d_{\text{P}})\pi$ back donations is calculated, leading to a total overlap population PO twice that of PB or PF. Summarizing, the oxygen ligand can be considered a strong σ acceptor and a much better π donor than the borine group, the bonds PF and PB are approximately single, and PO is best described as an axially symmetric double bond. Taken as a whole, the crude approach (16) proves to be a reasonable concept to deal with the complicated charge distribution in F_3PO called 'multiple phosphorus oxygen bond'.

From among other PE spectroscopic investigations of phosphorus compounds X_3PA^{53} the isoelectronic series of trimethylphosphine adducts⁵⁴ presented in Figure 13 is chosen as a rounding-off example to trace the electronic changes exercised by the different acceptor ligands. Without entering into details^{54, 55}, it is interesting simply to follow the PE band patterns⁵⁴.

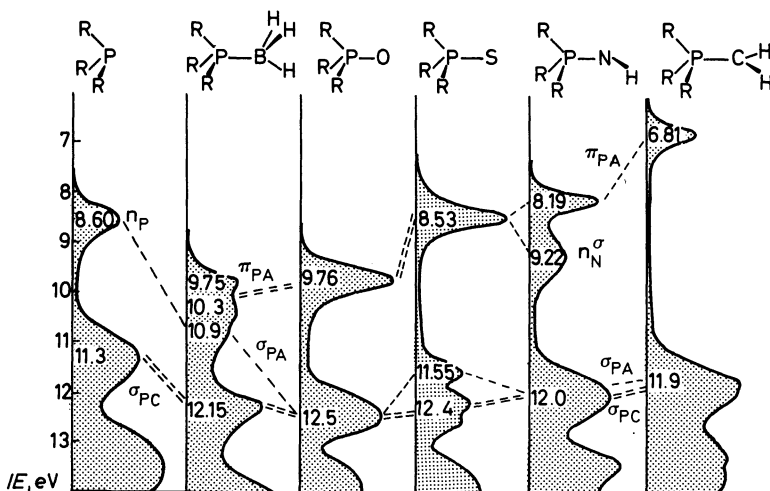


Figure 13. PE band patterns 6-13 eV for the isoelectronic series $(\text{H}_3\text{C})_3\text{P}-\text{A}$ with acceptors $\text{A} = \text{BH}_3, \text{O}, \text{S}, \text{NH}$ or CH_2 ⁵⁴.

Starting from trimethylphosphine, the PE spectrum of which is fully reproduced in *Figure 8*, on adduct formation the $\sigma_{\text{PC}}(\text{e})$ ionization energies are increased as expected (*Figure 12*). Again, attachment of another nuclear potential to the n_{p} electron pair (16) generates the σ_{PA} bond: thus, the stabilization $n_{\text{p}} \rightarrow \sigma_{\text{PB}}$ amounts to only half that of $n_{\text{p}} \rightarrow n_{\text{PO}}$, and in R_3PS the corresponding PE band moves out of the hill of overlapping ionizations (*Figure 13*). Most fascinating, however, is the movement of the 'multiple bond' ionization: the two PE bands of R_3PBH_3 , doubled due to Jahn–Teller distortion of the radical cation resulting upon electron removal from the degenerate orbitals of predominant σ_{BH} character, coalesce into one band of double intensity for π_{PO} . Lowered by about 1.2 eV, π_{PS} comes next. Removal of degeneracy on symmetry reduction $\text{C}_{3\text{v}} \rightarrow \text{C}_s$ leads to two single PE bands for the phosphine imine, assigned to the nitrogen electron pair n_{N}^{σ} incorporated into the σ skeleton and the perpendicular π_{PN} system. Finally, a record low ionization energy of only 6.81 eV is reached for the ylide π_{PC} (*Figure 13*), corresponding to electron ejection from an orbital of considerable 'carbanion' character⁵⁵.

Except for trimethyl phosphine oxide⁵⁶, no *ab initio* calculations are available for the other compounds listed in *Figure 13*; the probable reason is missing structure determinations rather than computational expenses for the 14 to 17 atom molecules. Because satisfying correspondence between *ab initio* and EHMO atomic charges and overlap populations is reported for phosphorus ylides⁵⁷, analogous calculations have been carried out⁵⁴ yielding e.g. for $(\text{H}_3\text{C})_3\text{PO}$:

	H	C	P	O	
<i>ab initio</i> ⁵⁶	+0.18	-0.61	+0.27	-0.14	
				1.47	
EHMO ⁵⁴	+0.04	-0.14	+1.11	-1.04	(18)
				1.04	
CNDO mod. ⁵⁴	+0.04	-0.12	+0.43	-0.43	
				1.03	

Comparison with the *ab initio* values seems not too convincing, although especially the modified CNDO version⁵⁸, reparametrized to reproduce PE ionization sequences, usually calculates dipole moments in rather good agreement with the experimental ones^{31,59}. The conclusion to be drawn is that in general—not questioning⁵⁷—the results of semi-empirical calculations should not be overemphasized. And, to end the discussion of the complicated charge distribution (16) in 'phosphine adducts', it therefore has to be pointed out that in spite of what has been achieved by the combined efforts of PE spectroscopy and MO calculations⁶⁰, there still remain many puzzles to be solved.

For example, of interest with regard to multiple bonding and charge distribution in phosphorus compounds might be another contribution from the Frankfurt photoelectron spectroscopy group⁶¹, which concerns the 'obliteration' of the benzene π system in trimethyl phosphorus benzylidene. As discussed before (cf. (13) and *Figure 9*), substituents in 1- or 1,4-position of the six-membered ring will shift only the symmetric π_s of the benzene $\pi(\text{e}_{2\text{g}})$ orbitals and will leave the antisymmetric π_{as} unperturbed. Therefore,

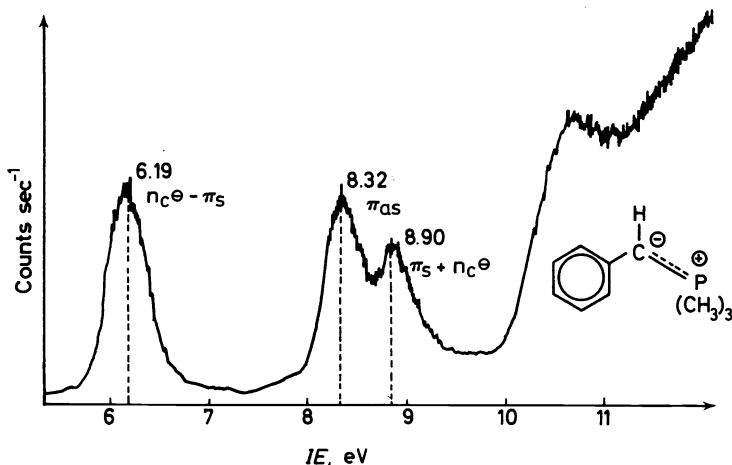


Figure 14. Expanded record 5–12 eV of the He(I) photoelectron spectrum of trimethyl phosphorus benzylidene⁶¹, calibrated with the $^2P_{3/2}$ xenon line at 12.13 eV.

the PE band assigned to electron removal from π_{as} is generally observed at about 9.2 eV, the first ionization potential of benzene itself. For the phenyl-substituted ylide, however, no PE band at all can be detected between 9 and 10.5 eV (Figure 14).

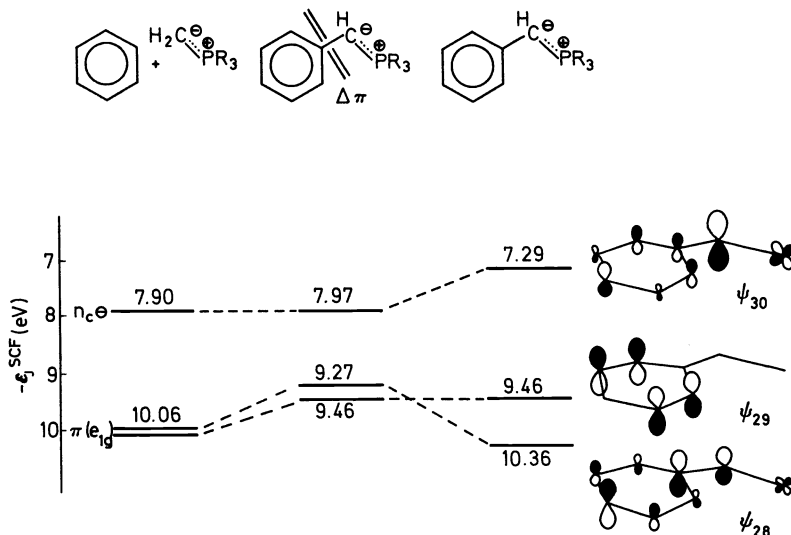


Figure 15. CNDO/2 correlation diagram for the highest occupied orbitals of the parent compounds, benzene and trimethyl phosphorus methylene, and of benzylidene, without ($\Delta\pi$) or with (π) interactions

To solve the puzzle of the 'vanished' benzene π ionization and to assign the benzyldiene PE spectrum, various courses were pursued. Calculations using a modified CNDO/2 version, which had been reparametrized to achieve optimum fit to PE data⁵⁸, yielded for the three highest occupied orbitals ψ_{30} , ψ_{29} and ψ_{28} the diagrams represented in *Figure 15*. Obviously, all are of π symmetry, and their sequence $n_C^\ominus (-\pi_s)$, $-\pi_{as}$, $\pi_s (+n_C^\ominus)$ meets the expectation from qualitative perturbation arguments as used previously, Scheme (13). Furthermore, the nodal plane through opposite ring centres in the anti-symmetric benzene π orbital is conserved in ψ_{29} , at least for the planar geometry assumed above. The CNDO/2 correlation diagram (*Figure 15*) also offers information as regards inductive and conjugational orbital movement on coupling of the parent systems: setting the corresponding off-diagonals in the CNDO/2 Hartree-Fock matrix identical to zero³¹, all π interactions between the six-membered ring and the ylide moiety can be cut off. This results in a destabilization of both benzene π orbitals; π_{as} being shifted as well, though a little less than π_s . Switching on the π interactions reverses their order; almost exclusively mixing the 'carbanion' orbital n_C^\ominus with π_s . Therefore, the raising of the second orbital, π_{as} , relative to the benzene π system can be considered to reflect the extreme inductive perturbation of the benzene π system by a 'carbanion' substituent.

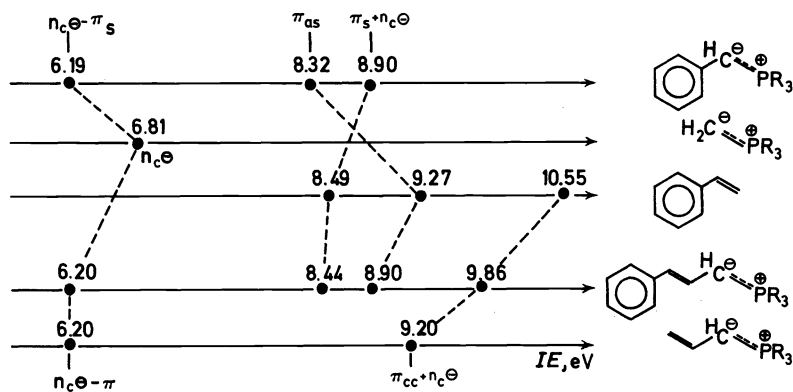
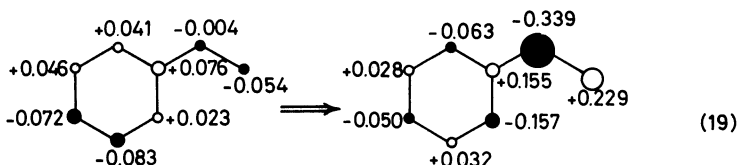


Figure 16. PE correlation diagram 6–11 eV for trimethyl phosphorus benzyldiene and appropriate model compounds^{61, 63}.

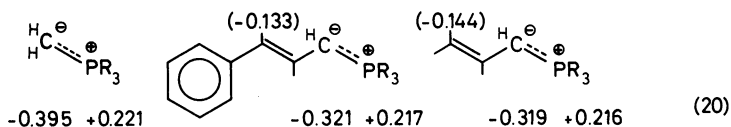
In view of the rather moderate quality of semi-empirical calculations, the modified CNDO/2 eigenvalues (*Figure 15*) correlate reasonably well with the PE ionization potentials (*Figure 14*) via the Koopmans theorem. In spite of its generally accepted validity, failures of the latter may be caused for instance by large charge redistribution in the resulting radical cation⁶⁵. Dealing with an ylide of presumably substantial carbanion character, therefore, its PE spectrum has been independently assigned by comparison with ionization potentials of chemically related compounds as shown in *Figure 16*.

There is hardly any doubt concerning the assignment of the benzyldiene low ionization energy PE band (*Figure 14*) to the ylide sub-unit as confirmed by the shift from 6.81 eV to 5.19 eV on conjugation (*Figure 16*). The styrene PE spectrum has been interpreted independently several times⁶⁴, and the band at 9.27 eV is concurringly attributed to electron ejection from orbital π_{as} , unshifted relative to benzene [*Figure 9* and Scheme (13)]. Substitution of the C=C double bond by the polarized C[⊖]—P[⊕] moiety should be accompanied by inductive shift as well as conjugational splitting. The amount of the latter can be roughly approximated by the decrease in the first ionization potential $\Delta IE_1 \approx 0.6$ eV relative to trimethylphosphorus methylene. Therefore, in trimethylphosphorus benzyldiene the band at 8.32 eV can only be assigned to π_{as} and the one at 8.90 eV only to π_s , conjugationally shifted by ~ 0.6 eV to higher ionization potential. Two underlying assumptions remain to be supported, namely the planarity of the benzyldiene π system and the tremendous inductive perturbation by the carbanionic substituent group. For both, the PE spectrum of the homologous cinnamylidene derivative offers some clues. To begin with, there is no steric reason for any twisting around the phenyl C—C ethylene bond, the P(CH₃)₃ group being quite remote. The second and third PE bands, although comparable in energy to those of the benzyldiene, have to be assigned the other way round, $\pi_s < \pi_{as}$, because the strongest π interaction will occur between the ethylene π_{CC} and the phenyl π_s (*Figure 16*: styrene $I_2 - I_1 = 0.78$ eV; $\Delta n_C^\ominus \sim 0.6$ eV). Nevertheless, as judged from the 9.27 \rightarrow 8.90 eV shift of π_{as} , there is a considerable perturbation of the benzene π system by the adjacent γ allylic centre of high electron density. Finally, the stunning inductive lift of the orbital with predominant π_{CC} contribution—shifted back by opposing π conjugation to 9.86 eV—becomes even more evident from the second ionization potential of trimethylphosphorus allylidene, found at 9.20 eV and unambiguously assigned to electron removal from the $\pi_{CC}(+n_C^\ominus)$ orbital: assuming an analogous π stabilization of +0.6 eV, the inductive lowering relative to ethylene ($IE_\pi = 10.51$ eV)—if separable—would amount to almost 2 eV!

In summary, substituting the terminal CH₂ group of styrene by a trimethylphosphorus group drastically distorts the original charge distribution and inflicts considerable benzylianium character as manifested also in the CNDO/2 total atomic charges:

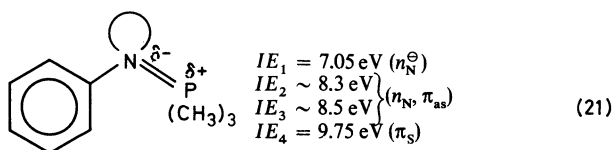


Comparable C[⊖]—P[⊕] charges have also been calculated for all the other ylide derivatives presented in *Figure 16*, with the charges at γ allylic centres given in parentheses:



The highest carbanion electron population results for the parent system, trimethylphosphorus methylene, and has been experimentally confirmed by ^{13}C n.m.r.⁶⁵: the chemical shift of the ylide carbon signal ($\delta = +200$ p.p.m.) resembles those of methyl grignard ($\delta = +207$ p.p.m.) or methyl lithium ($\delta = -206$ p.p.m.).

At least one consecutive question follows immediately: are the ylides a special case? The answer is no; for instance trimethylphosphorus phenyl-imide exhibits the same, though somewhat less exaggerated, features⁶³:



According to preliminary calculations⁶³ without optimized geometry, one major difference is the stronger π interaction, which shifts the π_{S} type orbital to 9.75 eV—back above its ionization potential in unsubstituted benzene, the starting point of this rather strange story.

CONCLUDING REMARKS

On a journey through the fascinating variety of phosphorus compounds, equipped with binoculars as supplied by the new method of measurement, photoelectron spectroscopy, and its close symbiosis with molecular orbital models, inevitably new aspects are added to the intriguing question of bonding in those molecules. Within the framework set up by the approach chosen, for sample, in the element P_4 the omnidirectional $3s_{\text{p}}$ orbitals contribute most to the σ skeleton, while phosphorus electron pairs as shown for phosphine and some derivatives are best described by $3p_{\text{p}}$ functions in linear combinations with varying σ contributions. Perturbation arguments are well suited to deal with substituent effects on π systems, including phosphorus groups or atoms, and no $3d_{\text{p}}$ inclusion seems really necessary. On the contrary, multiple bonding in phosphorus compounds like $\text{X}_3\text{P}=\text{Y}$ is still hard to rationalize satisfactorily and, hopefully, investigations on peculiar molecular systems like the ylides will offer some generalizable clues. Summarizing, photoelectron spectroscopy supplying all molecular ionization energies and, therefore, rendering possible via the Koopmans theorem a comparison with molecular orbital models, undoubtedly helps in understanding and rationalizing molecular properties. But as pointed out repeatedly, all kinds of models are at best reasonable approximations to the

reality of molecular states and 'actually, everything is much more complicated'.

REFERENCES

- ¹ Part XXXIX of Photoelectron Spectra and Molecular Properties; Part XXXVIII: H. Bock and P. Mollère, *J. Chem. Educ.* **51**, 506 (1974).
- ² Thesis, Dr W. Fuß, Frankfurt (1971).
- ³ W. Kutzelnigg, *Angew. Chem.* **85**, 564 (1973); *Angew. Chem. Internat. Ed.* **12**, 546 (1973).
- Among numerous reviews of photoelectron spectroscopy attention might be called to refs. 4-7:
- ⁴ D. W. Turner, C. Baker, A. D. Baker and C. R. Brundle, *Molecular Photoelectron Spectroscopy*. Wiley-Interscience: London (1970). The instrumental development and construction of a PE spectrometer are described. Literature is covered until 1969. Most important, the PE spectra of over a hundred molecules are given.
- ⁵ K. Siegbahn, C. Nordling, A. Fahlmann, R. Nordberg, K. Hamrin, J. Hedman, G. Johansson, T. Bergmark, S.-E. Karlsson, I. Lindgren and B. Lindberg, *ESCA: Atomic, Molecular and Solid State Structure Studied by means of Electron Spectroscopy*, Almqvist & Wiksells: Uppsala (1967) as well as K. Siegbahn, C. Nordling, G. Johansson, J. Hedman, P. F. Heden, H. Hamrin, U. Gelins, T. Bergmark, L. O. Werme, R. Mvnné and Y. Baer, *ESCA Applied to Free Molecules*, North Holland: Amsterdam (1969). Principles of high energy electron spectroscopy are illustrated by numerous examples, element ionization potentials are tabulated and compared with calculated values.
- ⁶ C. R. Brundle and M. B. Robin in F. C. Nachod and J. J. Zuckermann, *Determination of Organic Structures by Physical Methods*. Academic Press; New York (1971). Vol. III, pp. 1 ff. The available information from PE spectra and their interpretation is discussed with the aid of suitable examples.
- ⁷ H. Bock and B. G. Ramsey, 'Photoelectron spectra of nonmetal compounds and their interpretation by MO models', *Angew. Chem.* **85**, 773 (1973); *Angew. Chem. Internat. Ed.* **12**, 734 (1973).
- ⁸ T. Koopmans, *Physica*, **1**, 104 (1934); cf. also ref. 6 or E. Heilbronner 'Ups and downs in UPS' in the *Proceedings of the First International Congress of Quantum Chemistry* (edit. R. Daudel and B. Pullman), D. Reidel: Dordrecht/Holland (1974).
- ⁹ C. R. Brundle, N. A. Kuebler, M. B. Robin and H. Basch, *Inorg. Chem.* **11**, 20 (1972). The results of the *ab initio* calculation prove to be essentially in agreement with a semi-empirical calculation by K. Issleib and W. Grünter, *Theor. Chim. Acta*, **11**, 107 (1968).
- ¹⁰ S. Evans, P. J. Joachim, A. F. Orchard and D. W. Turner, *Internat. J. Mass. Spectrom. Ion Phys.* **9**, 41 (1972).
- ¹¹ H. Bock and W. Fuß, reported at the Euchem-Conference on 'Organic Chemistry of Phosphorus and of the Heavier Elements of Group Va' Elmau Castle/Germany (30 March-2 April 1971).
- ¹² H. Bock and W. Enßlin, *Angew. Chem.* **83**, 435 (1971), *Angew. Chem. Internat. Ed.* **10**, 404 (1971) or M. Beez, G. Bieri, H. Bock and E. Heilbronner, *Helv. Chim. Acta*, **56**, 1028 (1973).
- ¹³ Cf. e.g. E. Heilbronner and H. Bock, *Das HMO-Modell und seine Anwendung*, Vol. I to III. Verlag Chemie/Weinheim (1969-1970).
- ¹⁴ W. C. Price and A. W. Potts in *Molecular Spectroscopy 1971*, edit. P. Hepple, Institute of Petroleum, London (1972), p 42; cf. also *Proc. Roy. Soc. (London)*, **A326**, 181 (1972).
- ¹⁵ J. P. Maier and D. W. Turner, *J. Chem. Soc. Faraday II*, **68**, 11 (1972).
- ¹⁶ A neon PE spectrum of PH₃ is reported by G. R. Branton, D. C. Frost, C. A. McDowell and I. A. Stenhouse. *Chem. Phys. Letters*, **5**, 1 (1970).
- ¹⁷ J. M. Lehn and B. Munsch, *Mol. Phys.* **23**, 91 (1972), cf. also M. Lehn, *Fortschr. Chem. Forsch.* **15**, 311 (1970).
- ¹⁸ L. J. Aarons, M. F. Guest, M. B. Hall and I. H. Hillier, *J. Chem. Soc. Faraday II*, **69**, 643 (1973); cf. also I. H. Hillier and V. R. Saunders, *Trans. Faraday Soc.* **66**, 240 (1970) or M. F. Guest, I. H. Hillier and V. R. Saunders, *J. Chem. Soc. Faraday II*, **68**, 867 (1972).
- ¹⁹ J.-B. Robert, H. Marsmann, L. J. Schaad and J. R. von Wazer, *Phosphorus*, **2**, 11 (1972) and literature quotations given therein.
- ²⁰ Cf. e.g. G. Herzberg, *Molecular Spectra and Molecular Structure*, Vol. II, D. van Nostrand: New York (1945), pp 164 and 222, or M. B. Robin *Higher Electronic States of Polyatomic Molecules*, Vol. I, Academic Press: New York (1974), chapter III/D.

- ²¹ Structures of representative group Va compounds are comparatively discussed e.g. in (a) 'Molecular structure by diffraction methods' *Chem. Soc. Spec. Rep.* Vol. I, London (1973), (b) R. J. Gillespie *Molecular Geometry*, Van Nostrand/Reinhold: London (1972), p. 138 f. or R. F. Hudson *Structure and Mechanism in Organophosphorus Chemistry*, Academic Press: London (1965).
- ²² Cf. the recent review by K. Mislow, *Trans. NY Acad. Sci.* **11**, 227 (1973) or A. Rank, L. C. Allen and K. Mislow, *Angew. Chem.* **82**, 453 (1970); *Angew. Chem. Internat. Ed.* **9**, 400 (1970) as well as literature quotations given in both.
- ²³ S. Elbel, H. Bergmann and W. Enßlin, *J. Chem. Soc. Faraday II*, **70**, 555 (1974).
- ²⁴ P. J. Bassett and D. R. Lloyd, *J. Chem. Soc. Dalton*, 248 (1972) and literature quotations given therein.
- ²⁵ A. W. Potts, H. J. Lempka, D. G. Streets and W. C. Price, *Phil. Trans.* **A59**, 268 (1970).
- ²⁶ I. H. Hillier, J. C. Marriott, V. R. Saunders, M. J. Ware, D. R. Lloyd and N. Lynaugh, *Chem. Commun.* 1586 (1970), cf. also ref. 18.
- ²⁷ I. H. Hillier, V. R. Saunders, M. J. Ware, P. J. Bassett, D. R. Lloyd and N. Lynaugh, *Chem. Commun.* 1316 and 1586 (1970); cf. also J. Müller, K. Fenderl and B. Mertschenk, *Chem. Ber.* **104**, 700 (1971).
- ²⁸ H. Bock and S. Elbel, reported at the Euchem-Conference on 'Organic Chemistry of Phosphorus and of the Heavier Elements of Group Va', Elmau Castle /Germany (30 March–2 April 1971), part of the *Diplomarbeit* of S. Elbel, University of Frankfurt (1971).
- ²⁹ S. Cradock, E. A. V. Ebsworth, W. J. Savage and R. A. Whiteford, *J. Chem. Soc. Faraday II*, **68**, 934 (1972).
- ³⁰ I. H. Hillier and V. R. Saunders, *J. Chem. Soc. A*, 2475 (1970).
- ³¹ W. Enßlin, H. Bock and G. Becker, *J. Amer. Chem. Soc.* **96**, 2757 (1974) and literature quoted.
- ³² G. Becker, H. Bock, S. Elbel, G. Fritz and H. Schäfer, unpublished results; preliminary communication, cf. *Chimia*, **26**, 251 (1972).
- ³³ H. Bock, P. Mollère, G. Becker and G. Fritz, *J. Organomet. Chem.* **61**, 113 and 127 (1973).
- ³⁴ R. Hoffmann, *Acc. Chem. Res.* **4**, 1 (1971).
- ³⁵ H. Bock, G. Wagner and J. Kroner, *Tetrahedron Letters*, **40**, 3713 (1971) and *Chem. Ber.* **105**, 3850 (1972).
- ³⁶ J. P. Maier and T. W. Turner, *J. Chem. Soc. Faraday II*, 521 (1973); cf. also D. G. Streets, W. E. Hall and G. P. Ceasar, *Chem. Phys. Letters*, **17**, 90 (1972).
- ³⁷ H. Bock and S. Elbel, cf. ref. 28.
- ³⁸ W. Schäfer and A. Schweig, *Angew. Chem.* **84**, 898 (1972), *Angew. Chem. Internat. Ed.* **11**, 836 (1972).
- ³⁹ T. P. Debies and J. W. Rabelais, *Inorg. Chem.* **13**, 308 (1974).
- ⁴⁰ C. Batich, E. Heilbronner*, V. Hornung, A. J. Ashe III, D. T. Clark, U. T. Cogley, D. Kilcast and I. Scanlan, *J. Amer. Chem. Soc.* **95**, 928 (1973), and literature quoted, especially for pyridine.
- ⁴¹ R. L. Kuzkowsky and A. J. Ashe, *J. Mol. Spectrosc.* **42**, 457 (1972).
- ⁴² G. Märkl, *Angew. Chem.* **78**, 907 (1966).
- ⁴³ W. Schäfer and A. Schweig, together with H. Oehling, *Angew. Chem.* **83**, 723 (1971); *Angew. Chem. Internat. Ed.* **10**, 656 (1971), with K. Dimroth, *Angew. Chem.* **84**, 636 (1972), *Angew. Chem. Internat. Ed.* **11**, 631 (1972) and with F. Bickelhaupt and H. Vermeer, *Angew. Chem.* **84**, 993 (1972), *Angew. Chem. Internat. Ed.* **11**, 924 (1972).
- ⁴⁴ R. L. DeKock and D. R. Lloyd 'Vacuum ultraviolet photoelectron spectroscopy of inorganic molecules' in *Advances in Inorganic Chemistry and Radiochemistry* (edited by H. J. Emeléus and A. G. Sharpe) Vol. XVI, Academic Press: New York (1974), pp 98 ff.
- ⁴⁵ T. E. Gier, *J. Amer. Chem. Soc.* **83**, 1769 (1961).
- ⁴⁶ D. C. Frost, S. T. Lee and C. A. McDowell, *Chem. Phys. Letters*, **23**, 472 (1973).
- ⁴⁷ J.-B. Robert, H. Marsmann, I. Absar and J. R. Van Wazer, *J. Amer. Chem. Soc.* **93**, 3320 (1971).
- ⁴⁸ P. J. Bassett, D. R. Lloyd, I. H. Hillier and V. R. Saunders, *Chem. Phys. Letters*, **6**, 253 (1970) as well as refs 18, 24, 26.
- ⁴⁹ D. C. Frost, F. G. Herring, K. A. R. Mitchell and I. A. Stenhouse, *J. Amer. Chem. Soc.* **93**, 1596 (1971).
- ⁵⁰ J. Goubeau and D. Köttgen, *Z. Anorg. Allg. Chem.* **360**, 182 (1968) and W. Sawodny, A. Fadani and K. Ballein, *Spectrochim. Acta*, **21**, 995 (1965).
- ⁵¹ I. H. Hillier and V. R. Saunders, *J. Chem. Soc. A*, 664 (1971), as well as refs 18, 24, 26, 48 and literature quotations in all of them.
- ⁵² M. Barker, J. A. Connor, M. F. Guest, I. H. Hillier and V. R. Saunders, *Chem. Commun.* 943 (1971).

- ⁵³ J. C. Bünzli, D. C. Frost and C. A. McDowell, *J. Electron Spectrosc.* **1**, 481 (1972/73), cf. also P. A. Cox, S. Evans, O. F. Orchard, N. V. Richardson and J. P. Roberts, *Disc. Faraday Soc.* **54**, 26 (1972) and extensive literature quotations given in both.
- ⁵⁴ H. Bock, S. Elbel, H. Schmidbaur and W. Vornberger, unpublished results, part of the *Thesis* of S. Elbel; cf. also ref. 55.
- ⁵⁵ K. A. Ostoja Starzewski, H. tom Dieck and H. Bock, *J. Organomet. Chem.* **65**, 311 (1974) and literature quotations, especially for ylides.
- ⁵⁶ I. H. Hillier and V. R. Saunders, *J. Chem. Soc. A*, 2475 (1971), cf. also ref. 18.
- ⁵⁷ I. Absar and J. R. Van Wazer, *J. Amer. Chem. Soc.* **94**, 2383 (1972) quoting R. Hoffmann, D. B. Boyd and S. Z. Goldberg, *J. Amer. Chem. Soc.* **92**, 3927 (1970).
- ⁵⁸ J. Kroner, D. Proch, W. Fuß and H. Bock, *Tetrahedron*, **28**, 1585 (1972).
- ⁵⁹ H. Stafast and H. Bock, *Chem. Ber.* **107**, 1882 (1974).
- ⁶⁰ Due to space limitations only part of PE publications on phosphorus compounds could be reviewed. For those interested in phosphorus/nitrogen chemistry at least the following reference to work on phosphonitrilic derivatives is given: G. R. Branton, C. E. Brion, D. C. Frost, K. A. R. Mitchell and N. L. Paddock, *J. Chem. Soc. A*, 151 (1970).
- ⁶¹ 'Photoelectron spectra and molecular properties, Part XL', K. A. Ostoja Starzewski, H. Bock and H. tom Dieck, *Angew. Chem.* **87**, 197 (1975); *Internat. Edit.* **14**, 173 (1975).
- ⁶² Cf. e.g. F. Brogli, P. A. Clark, E. Heilbronner and M. Neuenschwander, *Angew. Chem.* **85**, 414 (1973), *Angew. Chem. Internat. Ed.* **12**, 422 (1973) or additional references quoted in ref. 8.
- ⁶³ K. A. Ostoja Starzewski and H. Bock, unpublished.
- ⁶⁴ Cf. e. g. J. P. Maier and D. W. Turner, *J. Chem. Soc. Faraday Trans. II*, **69**, 521 (1973), or T. Kobayashi, K. Yokota and S. Nagakura, *J. Electron Spectrosc.* **2**, 449 (1973).
- ⁶⁵ H. Schmidbaur, W. Buchner and D. Scheutzow, *Chem. Ber.* **106**, 1251 (1974), cf. also K. Hildenbrand and H. Dreeskamp, *Z. Naturforsch.* **28b**, 226 (1973) or G. A. Gray, *J. Amer. Chem. Soc.* **95**, 7736 (1973).